REGULAR PAPER

Energy Optimisation For End Face Turning With Variable Material Removal Rate Considering the Spindle Speed Changes

Luoke Hu[1] · Wei Cai[2] · Lianjie Shu[3] · Kangkang Xu[4] · Hao Zheng[1] · Shun Jia[5]

Abstract

Many studies have approved that optimising the cutting parameters is effective for reducing the energy consumption of machining operations of machine tools. However, this technique to reduce the end face turning energy consumption (EFTEC), where the material removal rate is variable, has not received attention. Besides, the energy consumed for the spindle speed changes was ignored in previous research. Aiming to fill these gaps, an integrated EFTEC model is developed considering the spindle speed changes. In terms of optimisation, the EFTEC model is discretised according to the allowable accuracy of the machine tool. Simulated annealing is adopted to search for the optimal values of cutting parameters that lead to the minimum EFTEC. In the case study, nine parts with changing diameters and cutting depths are machined by a lathe (CK6153i). According to the experiments, simulated annealing has more than 96% probability of obtaining the global optima. The optimum achieves a 14.03% EFTEC reduction for a case. The relationship between the design parameters and the optimal cutting parameters is discussed. A case shows that 2.43% of the machining time increases suffer from the EFTEC optimisation.

Keywords Cutting parameters optimisation · End face turning · Machine tool energy · Variable cutting rate · Spindle speed change · Simulated annealing

Abbreviations

EC	Energy consumption [J]
EFTEC	End face turning energy consumption [J]
SA	Simulated annealing
SRS	Spindle rotation speed [rpm]
MRR	Material removal rate [cm³/s]

List of symbols

α_A	Spindle's angular acceleration [rad/s²]
α_D	Spindle's angular deceleration [rad/s²]

✉ Shun Jia
herojiashun@163.com

1. Key Laboratory of Advanced Manufacturing Technology of Zhejiang Province, State Key Laboratory of Fluid Power and Mechatronic Systems, School of Mechanical Engineering, Zhejiang University, Hangzhou 310027, China

2. College of Engineering and Technology, Southwest University, Chongqing 400715, China

3. Faculty of Business Administration, University of Macau, Macau 999078, China

4. School of Electromechanical Engineering, Guangdong University of Technology, Guangzhou 510006, China

5. Department of Industrial Engineering, Shandong University of Science and Technology, Qingdao 266590, China

A_1, A_2, A_3	First, second, and third feeding activities
C_1	Spindle acceleration from 0 to n
C_2	Spindle deceleration from n to 0
C_L	Coefficient in the tool life model
d	Required cutting depth [mm]
$d(t)$	Function of cutting depth against time [mm]
D_0	Diameter of the part [mm]
E_{eft}	Total EFTEC for single-pass end face turning [J]
E_{fa}	EC for feeding activities in single-pass end face turning [J]
E_{fa}^j	EC for the j-th feeding activity [J]
E_{mc}	Material-cutting EC in single-pass end face turning [J]
E_{sc}	EC for spindle speed changes in single-pass end face turning [J]
f	Feed rate [mm/r]
f_L, f_U	Lower and upper bounds of feed rates in material-cutting [mm/r]
F_{cut}	Material-cutting force when the fully cutting begins [N]
F_U	Maximum allowable cutting force [N]
j	Index for a feeding activity
k	Index for the iteration
K	Main angle of the cutter [°]

n	Spindle rotation speed in material-cutting [rpm]
n_{max}	Maximum allowable SRS of the machine tool [rpm]
N_L	Minimum required passes of end face turning within one tool life
P_0	Basic power of the machine tool [W]
P_{cut}	Machine tool power when the fully cutting begins [W]
P_{CS}	Coolant spray power [W]
$P_{mc}(t)$	Function of material-cutting power against time [W]
P_{SR}	Spindle rotation power [W]
P_U	Maximum available machine tool power [W]
P_{XF}^2	X-axial feeding power for the second feeding activity [W]
P_{XR}	X-axial rapid feeding power [W]
R_N	Nose radius of the cutter [mm]
t	Time variable [s]
t_0	Moment when the material-cutting begins
t_{ce}	Cutter entering duration in material-cutting [s]
t_{fc}	Fully cutting duration in material-cutting [s]
t_j	Time consumption of the machine tool for the j-th feeding activity [s]
t_{mc}	Total material-cutting duration for the end face turning [s]
t_{XR}^j	X-axial rapid feeding time for the j-th feeding activity [s]
t_{ZR}^j	Z-axial rapid feeding time for the j-th feeding activity [s]
T_L	Tool life model for end face turning [s]
T_s	Spindle's acceleration torque [N m]
$v(t)$	Function of cutting speed against time [m/min]
v_L, v_U	Lower and upper bounds of cutting speeds in the beginning of material-cutting [m/min]
v_{XR}	X-axial rapid feeding speed [m/min]
v_{ZR}	Z-axial rapid feeding speed [m/min]
w_L, y_L, x_L	Exponents in the tool life model
w_M, y_M, x_M	Exponents in the model of material-cutting power
w_Q, y_Q, x_Q	Exponents in the model of material-cutting force
ΔX_j	Relative distance between the start and the end of the j-th feeding activity in X-axis [mm]
ΔZ_j	Relative distance between the start and the end of the j-th feeding activity in Z-axis [mm]

1 Introduction

Sustainable manufacturing can bring economic and environmental benefits to manufacturing industry as well as human society [1]. To promote sustainable manufacturing, it is a complex and emerging problem to reduce the energy consumption (EC) for machining operations of machine tools [2]. Many effective techniques were employed to solve this problem [3], including energy-efficient design, process planning, and scheduling [4]. Among these techniques, cutting parameters optimisation is selected in this research for its effectiveness [5]. The investigation showed that 6–40% of EC was effectively reduced when selecting the appropriate schemes of cutting parameters at the process planning stage [6].

To realise the energy-efficient cutting parameters optimisation, an important prerequisite is to accurately develop the EC model for machining operations of machine tools [7]. Specifically, Zhou et al. [8] reviewed more than 20 EC models and suggested that the accuracy of existing models could be improved by the correlation analysis of machining conditions. To cope with uncertainties in machining conditions, Bhinge et al. [9] developed a data-driven EC model using Gaussian process regression and machine learning [10], and the accuracy of the proposed model was over 94%. To be more accurate, Shi et al. [11] assumed the additional power of the machine tool caused by metal cutting to be proportional to cutting power at the tool-tip, and the accuracy achieved over 97%. In these references, the optimisation techniques such as mathematic algorithms were not provided to minimise the EC. To bridge this knowledge gap, many related optimisation studies have been conducted for various machining operations [12]. For the external turning operations, the turning parameters were optimised to minimise the EC for cutting the 7075 aluminium alloy based on the response surface methodology [13], and the EC was reduced by 13.55%. With the data mining techniques, a two-stage knowledge-driven method was proposed to realise the energy-related optimisation of turning parameters for multiple machining configurations [14]. For the face milling operations, the effect of milling parameters on the EC was analysed, and an experiment approach was provided for minimising the EC for AISI 1050 carbon steel [15]. To further improve the energy efficiency of milling operations, the embodied EC of materials was considered [12], and the specific EC was reduced by 19.59% for a case. Besides, the grinding, drilling, and threading parameters were optimised to reduce the EC for grinding [16], drilling [17], and threading [18] operations, respectively.

The aforementioned research only focuses on the machining operations whose material removal rate (MRR)

is constant [19]. Taking external turning operations as example, all cutting parameters including cutting speed, feed rate, and cutting depth remain unchanged during material-cutting [20]. Therefore, the MRR and cutting power are constant. In actual production, the machining operations whose MRR is variable are widely used, such as end face turning, grooving, and chamfering. As shown in Figs. 1 and 2, taking end face turning as example, the cutting speed and depth change with time during material-cutting, thereby leading to the dynamic change of MRR and cutting power. When the MRR is variable, the power characteristic is complicated. To the best of the authors' knowledge, the cutting parameters optimisation has not been conducted for the EC with variable MRR. An investigation suggested that the end face turning consumes considerable energy when machining a part [21]. In this study, single-pass end face turning is focused. The aim is to minimise the end face turning energy consumption (EFTEC) by optimising the cutting parameters.

The first step towards solving the optimisation problem is to develop the EFTEC model. The EFTEC is divided to three portions: the material-cutting EC, the EC for feeding activities, and the EC for spindle speed changes [22]. The material-cutting EC represents the additional EC of the machine tool for removing the materials to get the feature of end face [23]. The EC for feeding activities represents the EC of the machine tool for completing the tool path required by the end face turning without material removal [24]. The EC for spindle speed changes represents the EC of the machine tool for accelerating the spindle from 0 to

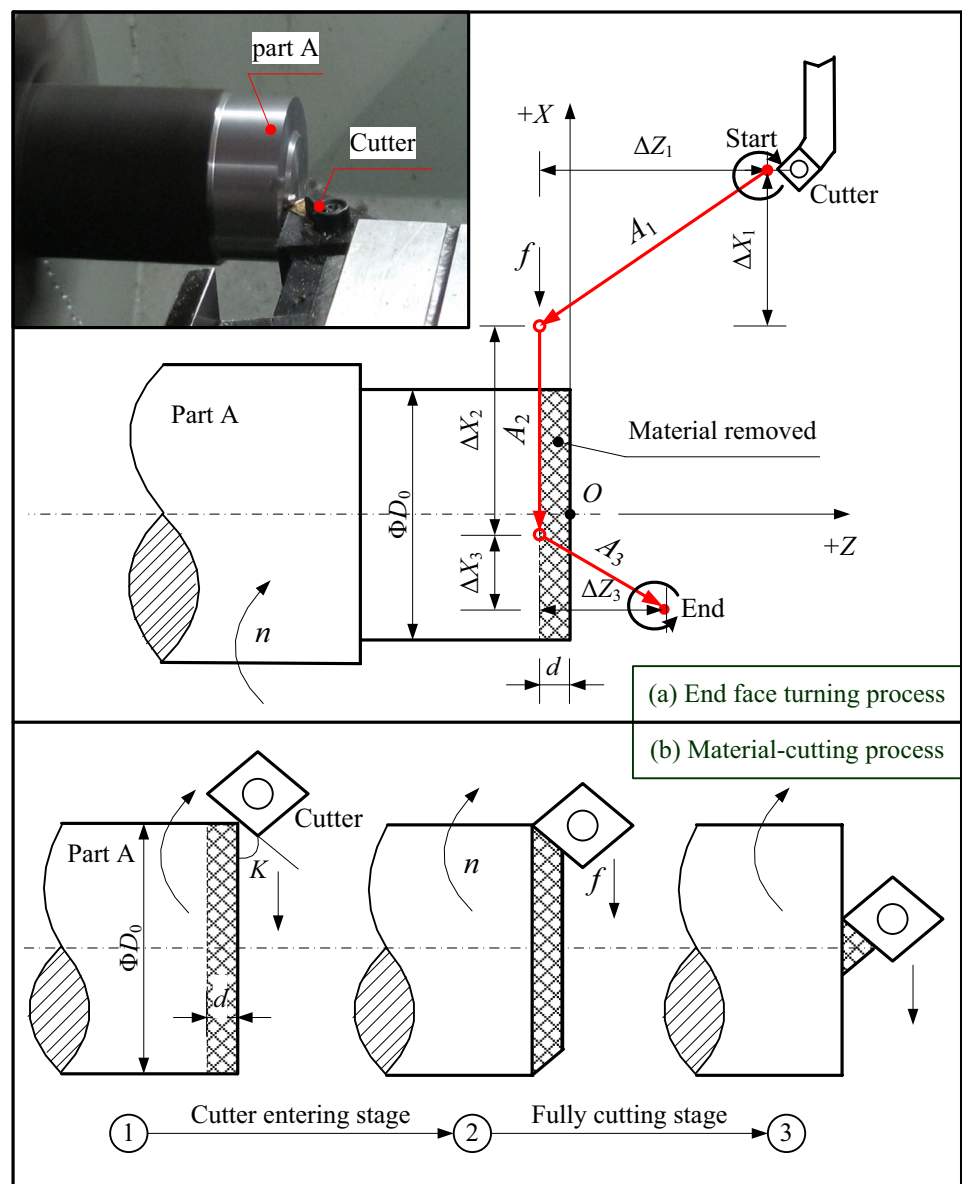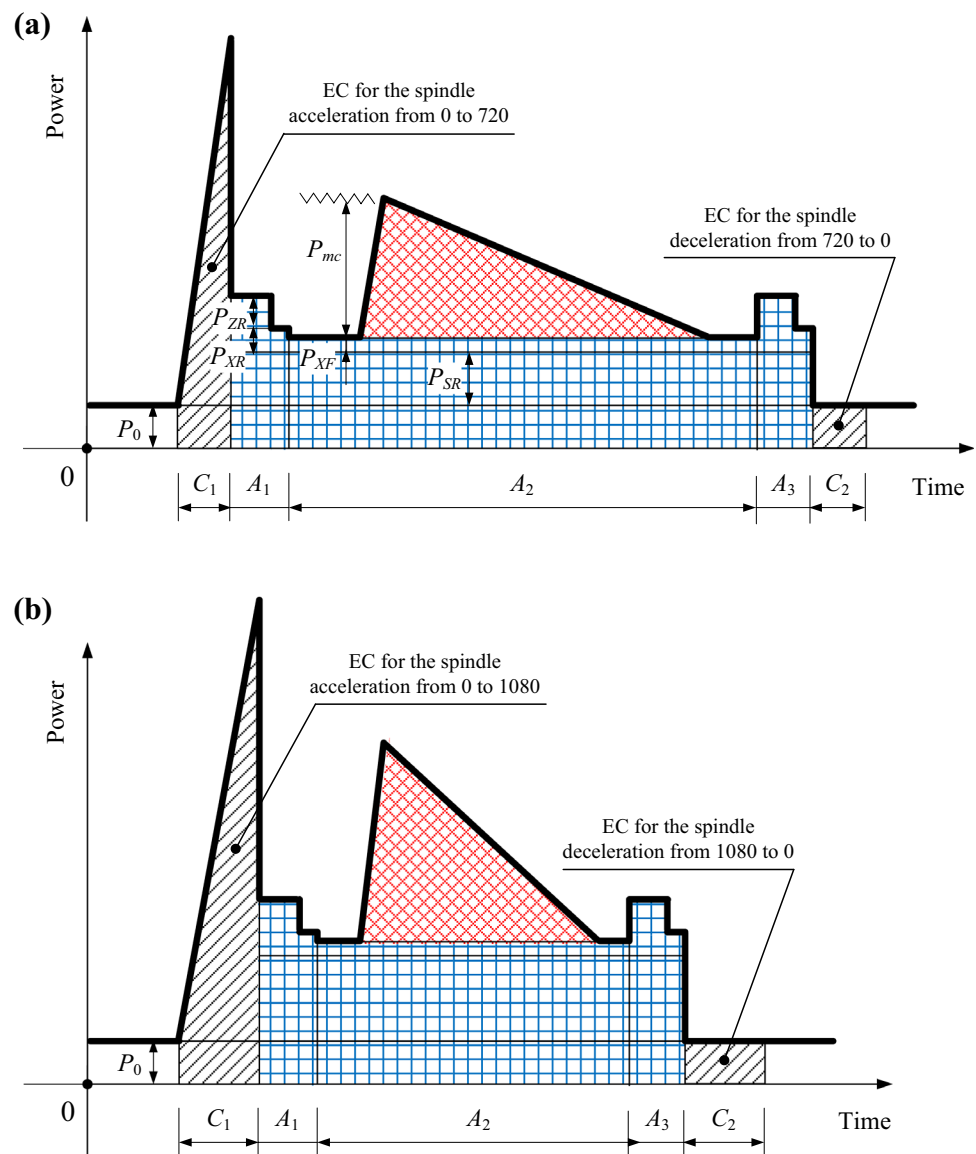**Fig. 1** End face turning operations for part A

Fig. 2 Power curves of the machine tool based on two schemes: **a** 720 rpm and 0.25 mm/r; **b** 1080 rpm and 0.25 mm/r. The forward slashes areas denote the EC for spindle speed changes, the blue grids areas denote the EC for feeding activities, and the red nets areas denote the material-cutting EC

required spindle rotation speed (SRS) and decelerating the spindle from required SRS to 0 [25]. Generally, the EC for spindle speed changes accounts for 5% of the total machining EC [25], but it has not received attention in the existing cutting parameters optimisation. The material-cutting EC model for end face turning was developed by Jia et al. [21] with fully reflecting the dynamic changing cutting power characteristics. The experiment was conducted to acquire the fitting coefficients and exponents [21]. The case study showed that the accuracy of the proposed model is 95.0%. The accurate EC models for feeding activities and spindle speed changes were built by Hu et al. [25] to solve the operation sequencing problem.

Although the aforementioned three models can be referred to integrate the EFTEC model, the following important gaps and insufficiencies have motivated this

study. (1) The operation sequencing problem is discrete. However, our cutting parameters optimisation problem is continuous at intervals. Thus, the existing EC models for feeding activities and spindle speed changes should be modified to be suitable for our problem. (2) The algorithm for optimising the material-cutting EC of end face turning has not been provided by Jia et al. [21], which restricts the energy reduction. (3) The optimisation of material-cutting EC can result in the increase of EC for feeding activities and spindle speed changes [26], and the total EFTEC may increase. Thus, the trade-off among three portions of EC should be made to optimise the total EFTEC. (4) The effect of the design parameter (part diameter) on the selection of cutting parameters for minimising the EFTEC has not been considered. In sum, it is novel to optimise the EFTEC with variable MRR considering the spindle

speed changes, and the proposed solutions are the original contributions.

This paper aims to analyse the conflicts among the material-cutting EC, the EC for feeding activities, and the EC for spindle speed changes, and to develop the integrated EFTEC model based on the cutting parameters. Especially, the design parameter of the diameter is included in the EFTEC model. The required cutting depth is a constant for single-pass end face turning because the initial and finished lengths of the part have been given. Further, the optimisation method is used to search for the optimal cutting parameters that lead to the minimum EFTEC. The type of our EFTEC optimisation problem is continuous at intervals. Yusup et al. [27] reviewed five popular heuristic algorithms including simulated annealing (SA), genetic algorithm [28], particle swarm optimisation, ant colony optimisation, and artificial bee colony for solving this type of problem from 2007 to 2011, and validated that SA performed better than other algorithms in terms of the solution quality [29]. Based on experiments and tests, Hu et al. [30] verified that SA can obtain the global optimum in a short computation time when the SRS and feed rate are continuous at intervals. Thus, SA is selected and is compared with the enumeration method to verify its performance about solution quality and computation speed for solving the EFTEC optimisation problem.

This paper is further organised as follows. Section 2 investigates the effect of cutting parameters on the EFTEC. In Sect. 3, the EFTEC model is developed. Section 4 describes the application of SA for optimising the EFTEC. Section 5 shows a case study to demonstrate the EFTEC model and optimisation methods. Section 6 analyses and discusses the optimisation results. In Sect. 7, the conclusions and future research are given.

2 Problem Description

The effect of the change of cutting parameters on the EFTEC is investigated. For example, part A is machined by a lathe, as shown in Fig. 1. This explains the material-cutting EC, the EC for feeding activities, and the EC for spindle speed changes, and the conflict among them when changing the cutting parameters. The required cutting depth is d. To finish part A, two schemes of cutting parameters including SRS and feed rate can be employed: (a) 720 rpm and 0.25 mm/r; (b) 1080 rpm and 0.25 mm/r. Dry cutting is adopted. In Fig. 1a, the red arrowed lines represent the tool paths in end face turning. The acceleration and deceleration of the spindle are represented by "↻" and "↺", respectively. According to aforementioned two schemes, power curves of the lathe are illustrated in Fig. 2. The power curves are drawn based on the simulation module developed by He et al. [31].

Firstly, the machining activities are identified and classified. In single-pass end face turning, there are one material-cutting activity, three feeding activities (A_1, A_2, and A_3), and two spindle speed changes (C_1 and C_2), as shown in Fig. 1a. The feeding modes for the first, second, and third activities are rapid, normal, and rapid, respectively. The SRS for them is the same as that of material-cutting activity. The cutting parameters can affect the EC for all of these activities [32]. For example, the EC for both C_1 and C_2 will increase when increasing the SRS from 720 rpm to 1080 rpm. In Fig. 2, the forward slashes areas denote the EC for spindle speed changes, and the blue grids areas denote the EC for feeding activities, and the red nets areas denote the material-cutting EC. The sizes of these areas between Fig. 2a and b are compared. It shows that changing schemes of cutting parameters can lead to different values of the material-cutting EC, the EC for feeding activities, and the EC for spindle speed changes.

The possible conflicts among three portions of EC are explained. The SRS of the first scheme (720 rpm) is slower than that of the second scheme (1080 rpm). Thus, the material-cutting power for the first scheme is smaller while the material-cutting time is longer, as shown in Fig. 2. The material-cutting EC model is required to calculate and compare the values of material-cutting EC between two schemes. As shown in Fig. 1b, the material-cutting process is divided into cutter entering stage (①⟶②) and fully cutting stage (②⟶③) with variable MRR, which increases the material-cutting EC modelling complexity. Since the low SRS requires the less spindle rotation power, the EC of A_1 and A_3 for the first scheme is smaller than that of the second scheme, as shown in Fig. 2. The EC of C_1 and C_2 for the first scheme is also smaller because the low SRS consumes the less EC [33]. However, the EC of A_2 for the first scheme is greater than that of the second scheme because the normal feeding time is 50% [(1080-720)/720] longer with consuming more basic energy of the machine tool [34]. Thus, the trade-off between the EC for feeding activities and the EC for spindle speed changes should be made when selecting the SRS. If the EC for spindle speed changes was neglected, the results would be skewed. This case suggests the requirement of developing an integrated EFTEC model and optimising the cutting parameters to achieve the minimum EFTEC. Especially, more feeding time reduction for A_2 can benefit from the second scheme if the diameter of part (D_0) is increased. The feeding time affects the EFTEC. Therefore, the design parameter of diameter is included in the EFTEC model.

3 Modelling

3.1 Objective Function

The EFTEC model for single-pass end face turning is developed. As shown in Fig. 2, the EFTEC is comprised

of the material-cutting EC, the EC for feeding activities, and the EC for spindle speed changes. Hence, the objective function of the model is expressed as:

$$\text{Minimise } E_{\text{eft}} = E_{\text{mc}} + E_{\text{fa}} + E_{\text{sc}} \tag{1}$$

where E_{eft} is the total EFTEC for single-pass end face turning [J], E_{mc} is the material-cutting EC [J], E_{fa} is the EC for feeding activities [J], and E_{sc} is the EC for spindle speed changes [J]. They are modelled as follows.

(1) Material-cutting EC (E_{mc})

The material-cutting power for end face turning varies with time, as shown in Fig. 2. Thus, E_{mc} is modelled as:

$$E_{\text{mc}} = \int_0^{t_{\text{mc}}} P_{\text{mc}}(t)dt \tag{2}$$

where t_{mc} is total material-cutting duration for the end face turning [s], t is the time variable [s], and $P_{\text{mc}}(t)$ is function of material-cutting power against time [W]. The material-cutting duration is divided into cutter entering duration and fully cutting duration, as shown in Fig. 1b. According to Jia et al. [21], t_{mc} is modelled as:

$$\begin{cases} t_{\text{mc}} = t_{ce} + t_{fc} \\ t_{ce} = \frac{d \times \cot K}{n \times f / 60} \\ t_{fc} = \frac{D_0/2 - d \times \cot K}{n \times f / 60} \end{cases} \tag{3}$$

where t_{ce} is cutter entering duration [s], t_{fc} is fully cutting duration [s], d is required cutting depth [mm], K is main angle of the cutter [°], n is SRS in material-cutting [rpm], f is feed rate [mm/r], and D_0 is diameter of the part [mm].

According to Jia et al. [21], a multiple regression equation that has an accuracy of 95% is employed to model the $P_{mc}(t)$, as follows:

$$P_{\text{mc}}(t) = C_M \cdot v(t)^{w_M} \cdot f^{y_M} \cdot d(t)^{x_M} \tag{4}$$

$$v(t) = \frac{\pi \times n}{1000} \left(D_0 - \frac{2 \times f \times n}{60} \times t \right) \tag{5}$$

$$d(t) = \begin{cases} d \times t/t_{ce}, & 0 \le t < t_{ce} \\ d, & t_{ce} \le t < t_{\text{mc}} \end{cases} \tag{6}$$

where C_M is coefficient in the model of material-cutting power, $v(t)$ is function of cutting speed against time [m/min], $d(t)$ is function of cutting depth against time [mm], and w_M,

y_M, and x_M are exponents in the model of material-cutting power, respectively.

(2) EC for feeding activities (E_{fa})

Single-pass end face turning has three feeding activities (A_1, A_2, and A_3) with the SRS of n, as shown in Fig. 1a, thus E_{fa} is expressed as:

$$E_{fa} = \sum_{j=1}^3 E_{fa}^j \tag{7}$$

where j denotes the index for a feeding activity and E_{fa}^j is EC for the j-th feeding activity [J]. Because there are two feeding modes (rapid and normal) in end face turning, two types of models for E_{fa}^j are provided. The feeding mode for A_1 and A_3 is rapid, and according to the model of Hu et al. [24], E_{fa}^j is expressed as:

$$E_{\text{fa}}^j = P_{\text{XR}} \times t_{\text{XR}}^j + P_{\text{ZR}} \times t_{\text{ZR}}^j + (P_0 + P_{\text{SR}}) \times t_j \tag{8}$$

$$\begin{cases} t_j = \max\left\{ t_{\text{XR}}^j, t_{\text{ZR}}^j \right\} \\ t_{\text{XR}}^j = \frac{60 \times \Delta X_j}{1000 \times v_{\text{XR}}} \\ t_{\text{ZR}}^j = \frac{60 \times \Delta Z_j}{1000 \times v_{\text{ZR}}} \end{cases} \tag{9}$$

$$P_{\text{SR}} = B_{\text{SR}} \times n + C_{\text{SR}} \tag{10}$$

where the symbols in Expressions (8, 9, 10) are explained as below. $P_{\text{XR}}, P_{\text{ZR}}$: X-axial and Z-axial rapid feeding power, respectively [W]. $t_{\text{XR}}^j, t_{\text{ZR}}^j$: X-axial and Z-axial rapid feeding time for the j-th feeding activity, respectively [s]. P_0: Basic power of the machine tool [W]. P_{SR}: Spindle rotation power [W]. t_j: Time consumption of the machine tool for the j-th feeding activity [s]. $\Delta X_j, \Delta Z_j$: Relative distances between the start and the end of the j-th feeding activity in X-axis and Z-axis, respectively [mm]. $v_{\text{XR}}, v_{\text{ZR}}$: X-axial and Z-axial rapid feeding speed, respectively [m/min]. $B_{\text{SR}}, C_{\text{SR}}$: Monomial coefficient and constant in the model of spindle rotation power.

The feeding mode for A_2 is normal, and the feeding direction is X-axial. Based on the model of Hu et al. [24], E_{fa}^2 is expressed as:

$$\begin{cases} E_{\text{fa}}^2 = \left(P_{\text{XF}}^2 + P_{\text{SR}} + P_{\text{CS}} + P_0 \right) \times \frac{60 \times \Delta X_2}{n \times f} \\ P_{\text{XF}}^2 = A_{\text{XF}} \times (n \times f)^2 + B_{\text{XF}} \times n \times f + C_{\text{XF}} \end{cases} \tag{11}$$

where P_{XF}^2 is X-axial feeding power for the second feeding activity [W], P_{CS} is coolant spray power [W], and A_{XF}, B_{XF},

and C_{XF} are quadratic coefficient, monomial coefficient, and constant, respectively, in the model of X-axial feeding power.

(3) EC for spindle speed changes (E_{sc})

For single-pass end face turning, the SRS accelerates from 0 to n and then decelerates to 0. According to Lv et al. [33], E_{sc} is modelled as:

$$\begin{cases} E_{sc} = E_{sc}^1 + E_{sc}^2 \\ E_{sc}^1 = \int_0^{\frac{2\pi n}{60\alpha_A}} \left[P_0 + B_{SR} \times \left(\frac{30\alpha_A t}{\pi} \right) + C_{SR} + T_s \times (\alpha_A t) \right] dt \\ E_{sc}^2 = P_0 \times \frac{2\pi(0-n)}{60\alpha_D} \end{cases}$$
(12)

where E_{sc}^1 is EC for accelerating the spindle from 0 to n [J], E_{sc}^2 is EC for decelerating the spindle from n to 0 [J], α_A and α_D are the spindle's angular acceleration and deceleration, respectively [rad/s^2], and T_s is the spindle's acceleration torque [N m].

The objective function can output the value of EFTEC when inputting the values of n and f.

3.2 Constraint Equations

The end face turning parameters should be selected with satisfying all constraint equations. By following Lu et al. [35], the constraint equations for the EFTEC model are developed considering the limits of cutting parameters, SRS, surface roughness, tool life [14], cutting force, and machine tool power. They are expressed as:

$$f_L \leq f \leq f_U$$
(13)

$$\begin{cases} v_L \leq v(t_0) \leq v_U \\ v(t_0) = \frac{\pi \times D_0 \times n}{1000} \end{cases} \xrightarrow{\text{Conversion}} \frac{1000 v_L}{\pi D_0} \leq n \leq \frac{1000 v_U}{\pi D_0}$$
(14)

$$n \leq n_{max}$$
(15)

$$\frac{f^2}{8R_N} \leq R_U$$
(16)

$$T_L = \frac{60 \cdot C_L}{v(t_{ce})^{w_L} \cdot f^{y_L} \cdot d^{x_L}} \geq N_L \times t_{mc}.$$
(17)

The cutting force and power at the moment when the fully cutting begins ($t = t_{ce}$) are selected to be restrained because the corresponding values are large [21]. The constraints are developed as:

$$F_{cut} = C_Q \cdot v(t_{ce})^{w_Q} \cdot f^{y_Q} \cdot d^{x_Q} \leq F_U$$
(18)

$$P_{cut} = P_{mc}(t_{ce}) + P_{XF}^2 + P_{SR} + P_{CS} + P_0 \leq P_U.$$
(19)

The notations in Constraints (13–19) are described as follows. f_L, f_U: Lower and upper bounds of feed rates in material-cutting [mm/r]. v_L, v_U: Lower and upper bounds of cutting speeds in the beginning of material-cutting [m/min]. t_0: Moment when the material-cutting begins. n_{max}: Maximum allowable SRS of the machine tool [rpm]. R_N: Nose radius of the cutter [mm]. R_U: Maximum allowable surface roughness [μm]. T_L: Tool life model for end face turning [s]. C_L: Coefficient in the tool life model. w_L, y_L, x_L: Exponents of cutting speed, feed rate, and cutting depth, respectively, in the tool life model. N_L: Minimum required passes of end face turning within one tool life. F_{cut}: Material-cutting force when the fully cutting begins [N]. C_Q: Coefficient in the model of material-cutting force. w_Q, y_Q, x_Q: Exponents in the model of material-cutting force. F_U: Maximum allowable cutting force [N]. P_{cut}: Machine tool power when the fully cutting begins [W]. P_U: Maximum available machine tool power [W].

4 Optimisation

After the EFTEC model is developed, SA is chosen as an optimisation method to get the optimal cutting parameters that lead to the minimum EFTEC. SA, proposed by Kirkpatrick et al. [36], is a probabilistic technique and meta-heuristic. It simulates the process of annealing in metallurgy to approximate the minimum internal energy (global optimum). To avoid premature convergence, the Metropolis criterion [37] about the acceptance of the inferior EFTEC value is incorporated. When the end temperature is reached, the optimal or near-optimal solutions are reported. Mahmoodpour and Masihi [38] presented the flowchart of SA.

According to the machine's allowable accuracy, the EFTEC model based on the cutting parameters is discretised. For example, the SRS is divided to 600, 601, 602, …, 1098, 1099, and 1100 when the SRS constraint is 600 rpm $\leq n \leq$ 1100 rpm. At the beginning, SA parameters are determined, including the initial and end temperatures, the temperature decrease function, and the length of Markov chain [39]. An initial solution including SRS and feed rate is random generated under the constraints (13–19). The candidate solution is generated through performing the random perturbations of SRS and feed rate on the last solution. This solution is checked to be accepted or rejected according to the EFTEC difference based on Expression (1) in each iteration. If the length of Markov chain is reached, the latest solution is returned with decreasing the temperature. Otherwise,

the new candidate solution is generated. This iteration process is repeated unless meeting a stopping condition. The stop condition can be the specified end temperature that is reached.

Although SA consumes a short time to reach a solution, it cannot guarantee the global optimum in all trials due to the nature of meta-heuristics. Enumeration method, which is a deterministic algorithm, is used as the benchmark for verifying SA's performance when minimising the EFTEC. Enumeration method lists all feasible schemes of SRS and feed rate under the Constraints (13)-(19) and then calculates the EFTEC according to Expressions (1–12) one by one [40]. By comparison, the scheme that leads to the minimum EFTEC is chosen as the optimum.

5 Case Study

The EFTEC optimisation for part A in Fig. 1 is demonstrated. Part A is made of 45#Steel. The required cutting depth d and diameter D_0 are 1.7 mm and 43.6 mm, respectively. Part A is scheduled to be processed by a computer numerical control lathe (CK6153i). The cutter to use for end face turning is SNMG120408N-GU-AC725 whose nose radius and main angle are $R_N = 0.8$ mm and $K = 45°$, respectively. The experiment method and the experiment device for collecting force and power data were presented in Lv et al. [41]. According to Jia et al. [21] and Hu et al. [30], Table 1 lists the CK6153i's parameters required for the EFTEC model. Because dry cutting is adopted, the coolant spray switch is OFF and corresponding power is $P_{CS} = 0$ W. Based on experiment measurements [41] and regression analysis [21], Table 2 provides the coefficients and exponents in the models of tool life and material-cutting force and power.

Table 2 Coefficients and exponents in the material-cutting models

Coefficient/exponent	Value
C_L	4.44×10^{12}
(w_L, y_L, x_L)	(6.568, 1.278, 0.20)
C_M	30.038
(w_M, y_M, x_M)	(1.035, 0.792, 1.039)
C_Q	2355
(w_Q, y_Q, x_Q)	(− 0.0724, 0.655, 0.902)

The process parameters for part A are obtained from the process files and listed in Table 3. The maximum allowable cutting force F_U is determined by the stability and strength of the lathe (CK6153i) and the cutter (SNMG120408N-GU-AC725) [42]. The maximum allowable surface roughness R_U is determined by the technical criteria of part A [42].

According to above data and Expressions (1)-(19), the EFTEC model for part A processed by CK6153i is developed in Table 4.

To optimise the EFTEC, both SA and enumeration method were developed on Dev C++5.11.0 software using the language C++. The computing platform is the same as that of Hu et al. [30]. According to the allowable accuracy of CK6153i, the intervals of n and f are set to 0.1 and 0.001 in algorithms, respectively. The global minimum EFTEC of 20166.5 J for part A was obtained by enumeration method. The computation time of enumeration method is 6.179 s, and the optimal cutting parameters are: $n = 594.6$ rpm and $f = 0.306$ mm/r. The values of SA parameters are: initial temperature = 200, end temperature = 0.001, temperature decrease function = 200×0.98^k, and length of Markov chain = 100. SA was run 50 times, and the global minimum EFTEC of 20166.5 J is returned in all trials. An average computation time of SA is 0.0957 s, and the optimal cutting parameters also are: $n = 594.6$ rpm and $f = 0.306$ mm/r.

Table 1 CK6153i's parameters required for the EFTEC model

Notation	[Unites]	Value
P_0	[W]	332.1
P_{CS} (ON, OFF)	[W]	(369.5, 0)
(B_{SR}, C_{SR})	–	(1.09, 41.12)
(A_{XF}, B_{XF}, C_{XF})	–	(4.24×10^{-6}, 0.017, − 1.63)
(α_A, α_D)	[rad/s^2]	(39.78, -38.79)
T_s	[N·m]	28.42
v_{XR}	[m/min]	4
v_{ZR}	[m/min]	8
P_{XR}	[W]	135.0
P_{ZR}	[W]	429.3
n_{max}	[rpm]	2000
P_U	[W]	7500

Table 3 Process parameters for part A

Notation	[Unites]	Value
d	[mm]	1.7
D_0	[mm]	43.6
ΔX_1	[mm]	13.2
ΔY_1	[mm]	26.7
ΔX_2	[mm]	28.8
ΔX_3	[mm]	42.0
ΔY_3	[mm]	26.7
(f_L, f_U)	[mm/r]	(0.090, 0.350)
(v_L, v_U)	[m/min]	(80, 195)
F_U	[N]	1280
N_L	–	12
R_U	[μm]	2.7

Table 4 The EFTEC model for part A processed by CK6153i

The objective function is:

minimise $E_{\mathrm{eft}} = E_{\mathrm{mc}} + E_{\mathrm{fa}} + E_{\mathrm{sc}} = \int_0^{t_{\mathrm{mc}}} P_{\mathrm{mc}}(t)dt + E_{\mathrm{fa}}^1 + E_{\mathrm{fa}}^2 + E_{\mathrm{fa}}^3 + E_{\mathrm{sc}}^1 + E_{\mathrm{sc}}^2$

Where:

$$\begin{cases} t_{\mathrm{mc}} = t_{\mathrm{ce}} + t_{\mathrm{fc}} \\ t_{\mathrm{ce}} = \frac{1.7 \times \cot 45°}{n \times f/60} \\ t_{\mathrm{fc}} = \frac{43.6/2 - 1.7 \times \cot 45°}{n \times f/60} \end{cases},$$

$$P_{\mathrm{mc}}(t) = \begin{cases} 30.038 \cdot \left[\frac{\pi \times n}{1000} \times \left(43.6 - \frac{2 \times f \times n}{60} \times t \right) \right]^{1.035} \cdot f^{0.792} \cdot \left(1.7 \times t/t_{ce} \right)^{1.039}, \ 0 \le t < t_{\mathrm{ce}} \\ 30.038 \cdot \left[\frac{\pi \times n}{1000} \times \left(43.6 - \frac{2 \times f \times n}{60} \times t \right) \right]^{1.035} \cdot f^{0.792} \cdot 1.7^{1.039}, \ t_{\mathrm{ce}} \le t < t_{\mathrm{mc}} \end{cases},$$

$E_{\mathrm{fa}}^1 = 135.0 \times \frac{60 \times 13.2}{1000 \times 4} + 429.3 \times \frac{60 \times 26.7}{1000 \times 8} + (332.1 + 1.09 \times n + 41.12) \times \frac{60 \times 26.7}{1000 \times 8}$,

$E_{\mathrm{fa}}^2 = \left[4.24 \times 10^{-6} \times (n \times f)^2 + 0.017 \times n \times f - 1.63 + 1.09 \times n + 41.12 + 0 + 332.1 \right] \times \frac{60 \times 28.8}{n \times f}$,

$E_{\mathrm{fa}}^3 = 135.0 \times \frac{60 \times 42.0}{1000 \times 4} + 429.3 \times \frac{60 \times 26.7}{1000 \times 8} + (332.1 + 1.09 \times n + 41.12) \times \frac{60 \times 42.0}{1000 \times 4}$,

$E_{\mathrm{sc}}^1 = \int_0^{\frac{2\pi n}{60 \times 39.78}} \left[332.1 + 1.09 \times \left(\frac{30 \times 39.78 \times t}{\pi} \right) + 41.12 + 28.42 \times 39.78 \times t \right] dt$,

$E_{\mathrm{sc}}^2 = 332.1 \times \frac{2\pi(0-n)}{60 \times (-38.79)}$.

The constraint equations are:

$0.090 \le f \le 0.350$,

$\frac{1000 \times 80}{\pi \times 43.6} \le n \le \frac{1000 \times 195}{\pi \times 43.6}$,

$n \le 2000$,

$\frac{f^2}{8 \times 0.8} \le 2.7$,

$\frac{60 \times 4.44 \times 10^{12}}{\left[\frac{\pi \times n}{1000} \times (43.6 - 2 \times 1.7 \times \cot 45°) \right]^{6.568} \cdot f^{1.278} \cdot 1.70.20} \ge 12 \times \frac{43.6/2}{n \times f/60}$

$2355 \cdot \left[\frac{\pi \times n}{1000} \times (43.6 - 2 \times 1.7 \times \cot 45°) \right]^{-0.0724} \cdot f^{0.655} \cdot 1.7^{0.902} \le 1280$,

$P_{\mathrm{mc}}(t_{\mathrm{ce}}) + 4.24 \times 10^{-6} \times (n \times f)^2 + 0.017 \times n \times f - 1.63 + 1.09 \times n + 41.12 + 0 + 332.1 \le 7500$
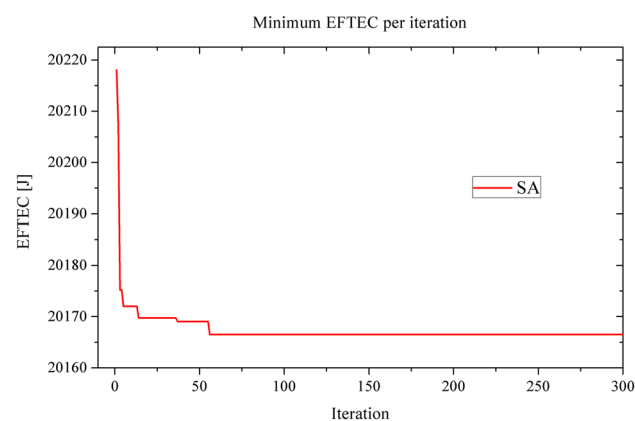

Fig. 3 A search process of SA for minimising the EFTEC of part A

Figure 3 shows a search process of SA for the global minimum EFTEC. For the case, SA converges in 300 iterations.

The performance of enumeration method and SA for part A is summarised in Table 5.

The methods are also tested on parts B, C, D, and E with the diameter D_0 of 43.5 mm, 75.4 mm, 107.2 mm, and 107.3 mm, respectively, when the cutting depth d is 1.7 mm. Furthermore, they are tested on parts F, G, H, and I with the cutting depth d of 1.5 mm, 1.6 mm, 1.8 mm, and 1.9 mm, respectively, when the diameter D_0 is 75.4 mm. By using SA and enumeration method, the results for optimising the EFTEC of these parts are listed in Table 5. It shows that the optimal SRS and feed rate are changed with the diameter and cutting depth, and the optimal SRS is between 534.7 rpm and 658.2 rpm. According to Table 5, SA has a 96% or more probability of getting the global optimal solutions.

By comparing the EFTEC in Table 5, it shows that the solution quality of SA is a little worse than that of enumeration method, but the computation time of SA is much less than that of enumeration method. For part B, the worst EFTEC obtained by SA is only 0.002%

Table 5 Results and performance of enumeration method and SA for case parts

Part names	Part A	Part B	Part C	Part D	Part E	Part F	Part G	Part H	Part I
Cutting depth [mm]	1.7	1.7	1.7	1.7	1.7	1.5	1.6	1.8	1.9
Diameter of the part [mm]	43.6	43.5	75.4	107.2	107.3	75.4	75.4	75.4	75.4
Enumeration									
Global minimum EFTEC [J]	20166.5	20122.5	38189.4	63693.1	63787.5	34635.2	35767.6	40803.6	43447.3
Optimal SRS [rpm]	594.6	585.4	622.2	578.4	578.4	536.3	534.7	639.5	658.2
Optimal feed rate [mm/r]	0.306	0.305	0.328	0.338	0.338	0.350	0.350	0.304	0.283
Computation time [s]	6.179	6.194	3.599	2.591	2.560	3.968	3.890	3.161	2.929
SA									
Minimum EFTEC achieved [J]	20166.5	20122.5	38189.4	63693.1	63787.5	34635.2	35767.6	40803.6	43447.3
Worst EFTEC in 50 trials [J]	20166.5	20122.9	38189.7	63693.1	63787.5	34635.3	35767.7	40803.9	43447.6
Median EFTEC of 50 trials [J]	20166.5	20122.5	38189.4	63693.1	63787.5	34635.2	35767.6	40803.6	43447.3
Probability of getting minimum	100%	98%	98%	100%	100%	96%	98%	98%	98%
Optimal SRS [rpm]	594.6	585.4	622.2	578.4	578.4	536.3	534.7	639.5	658.2
Optimal feed rate [mm/r]	0.306	0.305	0.328	0.338	0.338	0.350	0.350	0.304	0.283
Computation time [s]	0.0957	0.0953	0.0969	0.1087	0.1106	0.0895	0.0932	0.0992	0.1030

[(20122.9–20122.5)/20122.5] off from the global optimum, but the computation time of SA is 98.46% [(6.194–0.0953)/6.194] less than that of enumeration method. When the diameter increases from 43.5 mm to 107.3 mm, the computation time of enumeration method decreases from 6.194 to 2.560 s, but the computation time of SA slightly increases from 0.0953 to 0.1106 s. Among all cases, part E has the shortest computation time of enumeration method while the longest computation time of SA. For part E, the solution quality of SA is as good as that of enumeration method, but its computation time is 95.68% [(2.560–0.1106)/2.560] shorter than that of enumeration method. This verifies that SA can find good solutions in a short computation time. Thus, SA is recommended.

6 Discussion

In this section, the optimisation results are analysed. The relationship between the design parameters and the optimal SRS is described. Finally, the consequence of the EFTEC optimisation on the end face turning time is discussed.

6.1 Machining Energy Savings

The effect of our method in reducing the EFTEC is demonstrated. The traditional method of high SRS with medium feed rate serves as a benchmark to measure the energy savings [43]. The reason for selecting this method is that the high SRS can reduce the cutting time to improve the productivity while the medium feed rate can guarantee the surface quality of the workpiece [30]. The values of SRS and feed rate, generated by the traditional method,

are $n = 820$ rpm and $f = 0.25$ mm/r for parts A, C and I, where the corresponding values of EFTEC are 23828.1 J, 44421.9 J, and 46867.3 J, respectively. According to Table 5, the MRR of the traditional method for parts A, C, and I is higher than that of our method. Kara and Li [44] suggested that the higher MRR led to the less unit process EC. However, considerable energy savings benefit from our method even though the MRR of the traditional method is higher than ours. Specifically, the EFTEC is reduced by 15.37% [(23828.1–20166.5)/23828.1], 14.03% [(44421.9–38189.4)/44421.9], and 7.30% [(46867.3–43447.3)/46867.3] for parts A, C, and I, respectively, by using our method. The reason for causing the conflict is analysed. The high MRR contributes to minimising the material-cutting EC. The traditional method increases the MRR by increasing the SRS, thereby increasing the EC for spindle speed changes and feeding activities. For the three cases, the increase of the EC for spindle speed changes and feeding activities exceeds the reduction of the material-cutting EC. Therefore, the total EFTEC is not minimised when adopting the high MRR with the high SRS.

6.2 Design Parameters Effects

In previous energy optimisation, only the material-cutting EC is concerned while the EC for spindle speed changes is neglected. As a result, the upper bound of SRS is regarded as the optimum, and the optimal SRS decreases with increasing the diameter of the part due to the SRS constraint. In actual machining, the EC for spindle speed changes is inevitable [25]. After adding the EC, the optimal SRS fluctuates with the diameter when the cutting depth is 1.7 mm, as shown in Fig. 4. At first the optimal
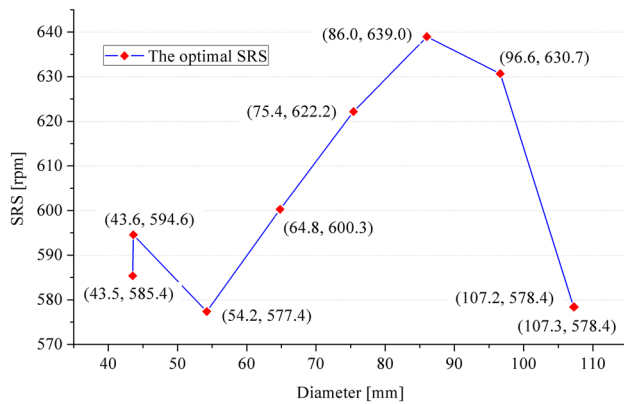
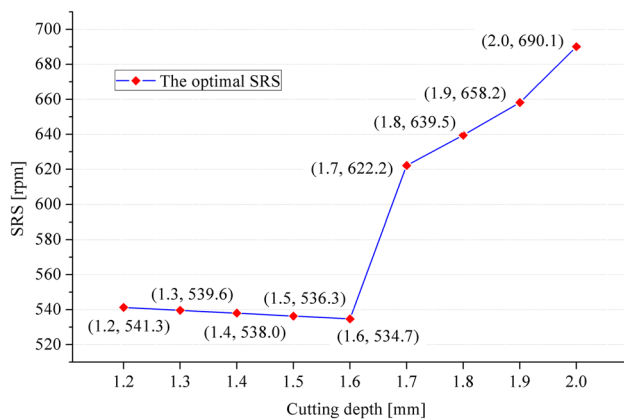**Fig. 4** The relationship between the diameter and the optimal SRS

Fig. 5 The relationship between the cutting depth and the optimal SRS

SRS sharply increases from 585.4 rpm (lower bound of SRS of part B) to 594.6 rpm when the diameter only increases from 43.5 to 43.6 mm. Then, the optimal SRS declines until 54.2 mm, bottoming out at 577.4 rpm. For the diameter from 43.5 to 54.2 mm, the lower bound of the SRS constraint (14) and the cutting force constraint (18) jointly cause the fluctuation of the optimal SRS. After that, the optimal SRS rises until 86.0 mm, reaching the highest point at 639.0 rpm. The increase of the optimal SRS is caused by the increase of the proportion of material-cutting EC. From this point onwards, the optimal SRS falls to 578.4 rpm (upper bound of SRS of part E) from 86.0 mm to 107.3 mm. The decrease of the optimal SRS is caused by the upper bound of the SRS constraint (14). For any part shorter than 43.5 mm and longer than 107.3 mm, the optimal SRS is the lower and upper bounds of SRS, respectively. Besides, the relationship between the cutting depth and the optimal SRS when the diameter is 75.4 mm is shown in Fig. 5. Specifically, the cutting depth between 1.2 mm and 1.6 mm experiences a slight

decrease in the optimal SRS from 541.3 rpm to the lowest point (534.7 rpm). After that, the optimal SRS goes up to 690.1 rpm from the cutting depth of 1.6–2.0 mm. The material-cutting EC becomes more dominant and causes the increase of the optimal SRS.

Overall, the relationship between the design parameters and the optimal SRS is not monotonously increasing or decreasing in the feasible solution space. For the next step, this relationship will be modelled. Thus, the optimal SRS can be directly calculated according to the values of diameter and cutting depth.

6.3 Machining Time Sacrifices

The effect of the end face turning energy optimisation on the end face turning time is discussed. The end face turning time based on the optimal cutting parameters of parts A ($n = 594.6$ rpm and $f = 0.306$ mm/r), C ($n = 622.2$ rpm and $f = 0.328$ mm/r), and I ($n = 658.2$ rpm and $f = 0.283$ mm/r) is 13.50 s, 17.53 s, and 18.98 s, respectively. By the aforementioned method of high SRS with medium feed rate, the cutting parameters of parts A, C, and I without considering the energy are generated. The end face turning time based on them ($n = 820$ rpm and $f = 0.25$ mm/r) is 13.63 s, 18.52 s, and 18.53 s for parts A, C, and I, respectively. Thus, 0.95% [(13.63-13.50)/13.63] and 5.35% [(18.52-17.53)/18.52] of the time reductions benefit from the energy minimisation of parts A and C, respectively. However, 2.43% [(18.98-18.53)/18.53] of the time increases suffer from the energy minimisation of part I, which verifies the conflicts between end face turning time and energy. If 2.43% of the time increases cannot cause the tardiness problem, the cutting parameters ($n = 658.2$ rpm and $f = 0.283$ mm/r) can be maintained for part I. Otherwise, the cutting parameters should be adjusted to optimise the trade-off between end face turning time and energy.

7 Conclusions

To realise sustainable manufacturing, reducing the machining EC is one of the challenges. It was approved that the cutting parameters optimisation is an effective approach for reducing the machining EC with constant MRR. However, this approach to reduce the machining EC with variable MRR did not receive attention. Besides, the EC for spindle speed changes was neglected in previous machining EC models. Thus, this paper develops the integrated EFTEC model including the sub-models of the material-cutting EC, the EC for feeding activities, and the EC for spindle speed changes. Especially, the design parameter of the diameter is included. In terms of optimisation, SA is employed and compared with enumeration method to verify its performance. In

sum, it is a novel contribution to optimise the EFTEC with variable MRR considering the trade-off among the reductions of three portions of EC.

A case study was performed. Nine parts with changing diameters and cutting depths are machined by a lathe (CK6153i). The experiments show that SA has more than 96% probability of finding the global optima. For a case, the worst EFTEC obtained by SA is only 0.002% off from the global optimum, but the computation time of SA is 98.46% less than that of enumeration method. Hence, SA is effective for solving the EFTEC optimisation problem. By using the proposed method, 15.37%, 14.03%, and 7.30% EFTEC are decreased for parts A, C, and I, respectively. According to experiment results, the optimal SRS fluctuates with the cutting depth and diameter. For a case, 2.43% of end face turning time increases suffer from the EFTEC optimisation. Thus, the trade-off between the reductions of EFTEC and end face turning time should be considered.

The EFTEC model is sensitive to the coefficients derived from the initial experiments as well as the combination of the machining conditions including the workpiece material, the cutting tool, and the lathe. It is questionable whether the conclusions from the case study apply to other machining conditions or not. More experiments and validations will be performed to discover the trends. Besides, this paper has not considered some other machining operations with variable MRR including grooving, chamfering, and hobbing [45]. They are required in machining and have energy-saving potentials. The EC for these operations will be modelled. Furthermore, the EC for the combination of end face turning and other machining operations will be optimised [46]. In actual machining, the time, quality, and cost should be controlled when reducing the EFTEC. To achieve the optimal trade-off among these objectives, multi-objective optimisation will be conducted. In the future, a software module based the proposed method will be developed to automatically provide with the optimal end face turning parameters.

Compliance with Ethical Standards

Conflict of Interest On behalf of all authors, the corresponding author states that there is no conflict of interest.

References

1. Lee, H., Song, J., Min, S., Lee, H., Song, K. Y., Chu, C. N., et al. (2019). Research trends in sustainable manufacturing: a review and future perspective based on research databases. *International Journal of Precision Engineering and Manufacturing-Green Technology, 6*(4), 809–819.

2. Lee, W., Kim, S. H., Park, J., & Min, B.-K. (2017). Simulation-based machining condition optimization for machine tool energy consumption reduction. *Journal of Cleaner Production, 150,* 352–360.

3. Jia, S., Tang, R., & Lv, J. (2016). Machining activity extraction and energy attributes inheritance method to support intelligent energy estimation of machining process. *Journal of Intelligent Manufacturing, 27*(3), 595–616.

4. Liu, N., Zhang, Y. F., & Lu, W. F. (2019). Improving energy efficiency in discrete parts manufacturing system using an ultra-flexible job shop scheduling algorithm. *International Journal of Precision Engineering and Manufacturing-Green Technology, 6*(2), 349–365.

5. Jang, D., Jung, J., & Seok, J. (2016). Modeling and parameter optimization for cutting energy reduction in MQL milling process. *International Journal of Precision Engineering and Manufacturing-Green Technology, 3*(1), 5–12.

6. Li, C., Xiao, Q., Tang, Y., & Li, L. (2016). A method integrating Taguchi, RSM and MOPSO to CNC machining parameters optimization for energy saving. *Journal of Cleaner Production, 135,* 263–275.

7. Jia, S., Yuan, Q., Cai, W., Lv, J., & Hu, L. (2019). Establishing prediction models for feeding power and material drilling power to support sustainable machining. *The International Journal of Advanced Manufacturing Technology, 100*(9), 2243–2253.

8. Zhou, L., Li, J., Li, F., Meng, Q., Li, J., & Xu, X. (2016). Energy consumption model and energy efficiency of machine tools: a comprehensive literature review. *Journal of Cleaner Production, 112,* 3721–3734.

9. Bhinge, R., Park, J., Law, K. H., Dornfeld, D. A., Helu, M., & Rachuri, S. (2017). Toward a generalized energy prediction model for machine tools. *Journal of Manufacturing Science and Engineering, 139*(4), 041013.

10. Kim, D., Kim, T. J. Y., Wang, X., Kim, M., Quan, Y., Oh, J. W., et al. (2018). Smart machining process using machine learning: a review and perspective on machining industry. *International Journal of Precision Engineering and Manufacturing-Green Technology, 5*(4), 555–568.

11. Shi, K., Ren, J., Wang, S., Liu, N., Liu, Z., Zhang, D., et al. (2019). An improved cutting power-based model for evaluating total energy consumption in general end milling process. *Journal of Cleaner Production, 231,* 1330–1341.

12. Chen, X., Li, C., Jin, Y., & Li, L. (2018). Optimization of cutting parameters with a sustainable consideration of electrical energy and embodied energy of materials. *The International Journal of Advanced Manufacturing Technology, 96*(1–4), 775–788.

13. Bhushan, R. K. (2013). Optimization of cutting parameters for minimizing power consumption and maximizing tool life during machining of Al alloy SiC particle composites. *Journal of Cleaner Production, 39,* 242–254.

14. Xiao, Q., Li, C., Tang, Y., Li, L., & Li, L. (2019). A knowledge-driven method of adaptively optimizing process parameters for energy efficient turning. *Energy, 166,* 142–156.

15. Campatelli, G., Lorenzini, L., & Scippa, A. (2014). Optimization of process parameters using a response surface method for minimizing power consumption in the milling of carbon steel. *Journal of Cleaner Production, 66,* 309–316.

16. Li, W., Winter, M., Kara, S., & Herrmann, C. (2012). Eco-efficiency of manufacturing processes: A grinding case. *CIRP Annals-Manufacturing Technology, 61*(1), 59–62.

17. Mori, M., Fujishima, M., Inamasu, Y., & Oda, Y. (2011). A study on energy efficiency improvement for machine tools. *CIRP Annals-Manufacturing Technology, 60*(1), 145–148.

18. Zhang, L., Zhang, B., & Bao, H. (2018). Cutting parameters optimization of thread turning oriented to low carbon and low noise. *Computer Integrated Manufacturing Systems, 24*(3), 639–648. **(in Chinese)**.

19. Wang, B., Liu, Z., Song, Q., Wan, Y., & Ren, X. (2020). An approach for reducing cutting energy consumption with ultra-high speed machining of Super Alloy Inconel 718. *International Journal of Precision Engineering and Manufacturing-Green Technology, 7*(1), 35–51.

20. Jiang, Z., Gao, D., Lu, Y., Kong, L., & Shang, Z. (2019). Quantitative analysis of carbon emissions in precision turning processes and industrial case study. *International Journal of Precision Engineering and Manufacturing-Green Technology*. https://doi.org/10.1007/s40684-019-00155-9.

21. Jia, S., Tang, R., Lv, J., Zhang, Z., & Yuan, Q. (2016). Energy modeling for variable material removal rate machining process: an end face turning case. *The International Journal of Advanced Manufacturing Technology, 85*(9–12), 2805–2818.

22. Hu, L., Peng, C., Evans, S., Peng, T., Liu, Y., Tang, R., et al. (2017). Minimising the machining energy consumption of a machine tool by sequencing the features of a part. *Energy, 121,* 292–305.

23. Hu, L., Tang, R., He, K., & Jia, S. (2015). Estimating machining-related energy consumption of parts at the design phase based on feature technology. *International Journal of Production Research, 53*(23), 7016–7033.

24. Hu, L., Liu, Y., Peng, C., Tang, W., Tang, R., & Tiwari, A. (2018). Minimising the energy consumption of tool change and tool path of machining by sequencing the features. *Energy, 147,* 390–402.

25. Hu, L., Liu, Y., Lohse, N., Tang, R., Lv, J., Peng, C., et al. (2017). Sequencing the features to minimise the non-cutting energy consumption in machining considering the change of spindle rotation speed. *Energy, 139,* 935–946.

26. Camposeco-Negrete, C. (2015). Optimization of cutting parameters using Response Surface Method for minimizing energy consumption and maximizing cutting quality in turning of AISI 6061 T6 aluminum. *Journal of Cleaner Production, 91,* 109–117.

27. Yusup, N., Zain, A. M., & Hashim, S. Z. M. (2012). Evolutionary techniques in optimizing machining parameters: Review and recent applications (2007–2011). *Expert Systems with Applications, 39*(10), 9909–9927.

28. Deng, Z., Lv, L., Huang, W., & Shi, Y. (2019). A high efficiency and low carbon oriented machining process route optimization model and its application. *International Journal of Precision Engineering and Manufacturing-Green Technology, 6*(1), 23–41.

29. Asokan, P., Saravanan, R., & Vijayakumar, K. (2003). Machining parameters optimisation for turning cylindrical stock into a continuous finished profile using genetic algorithm (GA) and simulated annealing (SA). *The International Journal of Advanced Manufacturing Technology, 21*(1), 1–9.

30. Hu, L., Tang, R., Cai, W., Feng, Y., & Ma, X. (2019). Optimisation of cutting parameters for improving energy efficiency in machining process. *Robotics and Computer-Integrated Manufacturing, 59,* 406–416.

31. He, K., Tang, R., Zhang, Z., & Sun, W. (2016). Energy consumption prediction system of mechanical processes based on empirical models and computer-aided manufacturing. *Journal of Computing and Information Science in Engineering, 16*(4), 041008.

32. Yoon, H., Lee, J., Kim, M. S., Kim, E., Shin, Y., Kim, S., et al. (2020). Power consumption assessment of machine tool feed drive units. *International Journal of Precision Engineering and Manufacturing-Green Technology, 7*(2), 455–464.

33. Lv, J., Tang, R., Tang, W., Liu, Y., Zhang, Y., & Jia, S. (2017). An investigation into reducing the spindle acceleration energy consumption of machine tools. *Journal of Cleaner Production, 143,* 794–803.

34. Lv, J. (2014). *Research on energy supply modeling of computer numerical control machine tools for low carbon manufacturing [dissertation]*. Hangzhou: Zhejiang University. **(in Chinese)**.

35. Lu, C., Gao, L., Li, X., & Chen, P. (2016). Energy-efficient multi-pass turning operation using multi-objective backtracking search algorithm. *Journal of Cleaner Production, 137,* 1516–1531.

36. Kirkpatrick, S., Gelatt, C. D., & Vecchi, M. P. (1983). Optimization by simulated annealing. *Science, 220*(4598), 671–680.

37. Tian, P., Ma, J., & Zhang, D. M. (1999). Application of the simulated annealing algorithm to the combinatorial optimisation problem with permutation property: An investigation of generation mechanism. *European Journal of Operational Research, 118*(1), 81–94.

38. Mahmoodpour, S., & Masihi, M. (2016). An improved simulated annealing algorithm in fracture network modeling. *Journal of Natural Gas Science and Engineering, 33,* 538–550.

39. Farzad, H., & Ebrahimi, R. (2017). Die profile optimization of rectangular cross section extrusion in plane strain condition using upper bound analysis method and simulated annealing algorithm. *Journal of Manufacturing Science and Engineering, 139*(2), 021006.

40. Gupta, R., Shishodia, K. S., & Sekhon, G. S. (2011). Optimization of grinding process parameters using enumeration method. *Journal of Materials Processing Technology, 112*(1), 63–67.

41. Lv, J., Tang, R., Jia, S., & Liu, Y. (2016). Experimental study on energy consumption of computer numerical control machine tools. *Journal of Cleaner Production, 112,* 3864–3874.

42. Sardinas, R. Q., Santana, M. R., & Brindis, E. A. (2006). Genetic algorithm-based multi-objective optimization of cutting parameters in turning processes. *Engineering Applications of Artificial Intelligence, 19*(2), 127–133.

43. Kumar, N. S., Shetty, A., Shetty, A., Ananth, K., & Shetty, H. (2012). Effect of spindle speed and feed rate on surface roughness of Carbon Steels in CNC turning. *Procedia Engineering, 38,* 691–697.

44. Kara, S., & Li, W. (2011). Unit process energy consumption models for material removal processes. *CIRP Annals-Manufacturing Technology, 60*(1), 37–40.

45. Cai, W., Li, L., Jia, S., Liu, C., Xie, J., & Hu, L. (2020). Task-oriented energy benchmark of machining systems for energy-efficient production. *International Journal of Precision Engineering and Manufacturing-Green Technology, 7*(1), 205–218.

46. Jackson, M. A., Van Asten, A., Morrow, J. D., Min, S., & Pfefferkorn, F. E. (2018). Energy consumption model for additive-subtractive manufacturing processes with case study. *International Journal of Precision Engineering and Manufacturing-Green Technology, 5*(4), 459–466.

Luoke Hu received the B.Eng. degree in industrial engineering from Zhejiang University of Technology, Hangzhou, China, in 2011, and the Ph.D. degree in industrial engineering from Zhejiang University, Hangzhou, China, in 2017. He was a visiting scholar with the Institute for Manufacturing, Department of Engineering, the University of Cambridge, Cambridge, U.K., from 2014 to 2015. He is currently a research associate with

the School of Mechanical Engineering, Zhejiang University, Hangzhou, China. His research interests include sustainable manufacturing, intelligent manufacturing, and energy optimisation.

Wei Cai received Ph.D. degree in mechanical engineering from Chongqing University, China, in 2018. Currently, he is a lecturer at Department of Mechanical Engineering, College of Engineering and Technology, Southwest University, Chongqing, China, and is a postdoctoral fellow at Department of Logistics and Maritime Studies, Faculty of Business, The Hong Kong Polytechnic University, Hung Hum, Kowloon, Hong Kong. His fields of interest are green manufacturing, sustainability evaluation and energy benchmarking.

Lianjie Shu received the B.Eng. degree in Mechanical Engineering and Automation from Xi'an Jiaotong University, Xi'an, China, in 1998, and the Ph.D. degree in Industrial Engineering and Engineering Management from the Hong Kong University of Science and Technology, Hong Kong, China, in 2002. He is currently a professor with the Faculty of Business Administration, University of Macau, Macau, China. His research interests include high-dimensional statistics, financial engineering, and statistical learning.

Kangkang Xu received his B.E. degree and Ph.D. degree in mechatronics engineering from Central South University, Changsha, China, in 2012 and 2017, respectively. He is currently a Lecturer with the School of Electromechanical Engineering, Guangdong University of Technology, Guangzhou, China. His research interests include distributed parameter system and intelligent modeling.

Hao Zheng received the B.S. degree in Mechanical Engineering from SouthWest JiaoTong University, Chengdu, China, in 2010, and the Ph.D. degree in Mechanical Engineering from Zhejiang University, Hangzhou, China, in 2017. He is affiliated with State Key Laboratory of CAD&CG and State Key Laboratory of Fluid Power and Mechatronic Systems, Zhejiang University, Hangzhou, China. His recent research interests include data-driven design, decision-making and optimization, multi-objective evolutionary algorithms and machine learning.

Shun Jia received the Ph.D. degree in industrial engineering from Zhejiang University, Hangzhou, China, in 2014. Currently, he is an associate professor at the Shandong University of Science and Technology. His fields of interest are sustainable design, low carbon manufacturing, and lean production.